Simulation of one dimensional open channel flows using the SPH model

Manoj Kumar Diwakar[1,*] and Pranab Kumar Mohapatra[2]

[1]Department of Civil Engineering, Malaviya National Institute of Technology Jaipur, Jaipur 302 017, India
[2]Discipline of Civil Engineering, Indian Institute of Technology Gandhinagar, Gandhinagar 382 355, India

In this study, shallow water equations with source terms were numerically solved using the smoothed particle hydrodynamics (SPH) method. The proposed model can incorporate the inflow and outflow boundaries. In addition, bed discontinuity was modelled using the fluid particles without any extra bed particles. Artificial viscosity to smoothen the numerical oscillations in the water surface profile was considered. The sensitivity and convergence analyses were used to determine the optimal model parameters. Seven different kinds of open channel flow in prismatic channels were simulated to demonstrate the model's capabilities. The numerical accuracy was quantified in terms of L_2 error norm. Comparison with earlier results shows that the SPH model can be used to compute steady and unsteady open channel flows with or without bed discontinuity.

Keywords: Hydraulics, open channel flow, shallow water equations, smoothened particle hydrodynamics.

TRADITIONALLY, open channel flows have been described by shallow water equations (SWEs), and varieties of such flows have been simulated using Eulerian-based models[1,2]. Some numerical models based on the Lagrangian approach have also been reported in the literature[3]. In the present study, a Lagrangian approach – smoothed particle hydrodynamics (SPH) – is employed to explore its capability to simulate open-channel flows using SWEs.

The SPH method is a Lagrangian and mesh-free method in which fluid elements are represented by particles that carry flow quantities such as mass, depth and velocity[4]. The motion of such particles is obtained by simulation of the advection of such fluid elements using kernels without the underlying mesh. The free surface does not require any specific treatment in SPH, and being a Lagrangian formulation, the mass is conserved. Excellent reviews of the SPH method are available in the literature[5–8]. A brief literature review on the simulation of open channel flows using the SPH method is presented here.

Monaghan[9] applied the SPH method to simulate several free surface problems such as the evolution of drop, dam break flow, formation of bore, etc. Swegle *et al.*[10] performed a stability analysis of the SPH method. Morris *et al.*[11] applied the SPH method to laminar incompressible flows. Bonet and Lok[12] studied the variational and momentum preservation aspects of the SPH formulation. Cummins and Rudman[13] introduced the incompressible SPH (ISPH) method to obtain better pressure distribution. Wang and Shen[4] studied one-dimensional inviscid dam break flows on a wet bed using the SPH model for SWEs. Inutsuka[14] introduced Riemann solver for the SPH method. Cha and Whitworth[15] presented a new formulation of SPH called the GPH (Godunov-type particle hydrodynamics). Rodriguez-Paz and Bonet[16] derived a corrected SPH formulation for SWEs from the variational formulation and studied idealized dam break flows. Hu and Adams[17] developed the multi-phase SPH method for incompressible flows. Grenier *et al.*[18] used the Hamiltonian approach to study open channel flows. De-Leffe *et al.*[19] used an anisotropic kernel with variable smoothing length and presented a different scheme based on the Riemann approach for shallow water coastal flows[20]. Chang *et al.*[21], and Kao and Chang[22] studied dam-break flows in realistic open channels using SWEs with the SPH formulation. Vacondio *et al.*[23] proposed a particle-splitting procedure to overcome the issue of poor resolution at small depths. They provided an enhanced formulation for shock capture and presented test cases with open boundaries[24]. Meister *et al.*[25] performed a Reynolds number sensitivity analysis of the SPH method for open channel flows. Voileau and Leroy studied the optimal time stepping in the ISPH method. Violeau and Rogers[8] reviewed the SPH method for free-surface flow problems. Sun *et al.*[26] improved the performance of the SPH method using a simple procedure and named it as δ plus-SPH model. Chang *et al.*[27] developed the 1D–2D coupled SPH-SWE model for open channel flow simulations in complicated geometries. Gu *et al.*[28] simulated the hydraulic jump on corrugated river channel beds using the SPH methodology. Hsu *et al.*[29,30] used the SPH model to simulate moving wet/dry fronts. Recently, Chang *et al.*[31] have presented a well-balanced SPH methodology for shallow water flows in open channels.

In the present study, a one-dimensional numerical model has been developed in the SPH framework for SWEs to simulate open channel flows in prismatic channels. The SWEs are solved using the SPH formulation[4]. Note that the source term in the SWEs is considered in the present model to account for channel-bed variation, whereas it was not considered by Wang and Shen[4]. The source term

*For correspondence. (e-mail: manoj.ce@mnit.ac.in)

was computed using the SPH formulation of Vacondio *et al.*[24] who used it taking into account extra bed particles. However, no extra bed particles were included in the present formulation to reduce the computational cost. The flow properties and channel-bed bathymetry were obtained using a single type of particle, considering both fluid and channel-bed properties at a single particle location. In this study, a standard force approach to solving the SWEs by treating the water depth equivalent to density was followed. Water elevation was calculated in the simulation, and water depth was obtained by subtracting the bed bathymetry. The momentum of fluid particles was obtained with the existing forces rather than kinetic and potential energies, which have been used in the variational approach of Vacondio *et al.*[24]. Seven different open channel flows were simulated to demonstrate the applicability of the present model.

SPH formulation for SWE

SWEs in the non-conservative form can be written as

$$\frac{Dh}{Dt} + h\nabla \cdot \mathbf{u} = 0, \tag{1}$$

and

$$\frac{D\mathbf{u}}{Dt} + \boldsymbol{g}\nabla h = \boldsymbol{g}(S_0 - S_\mathrm{f}), \tag{2}$$

where h, $\mathbf{u}$ and $\boldsymbol{g}$ represents water depth, velocity and acceleration due to gravity respectively. S_0 and S_f are bed and friction slope respectively, and D/Dt is the total derivative.

Using the SPH methodology, we can write the continuity and momentum equations of SWEs as[4]

$$\frac{Dh_i}{Dt} == -\sum_{j=1}^{N} \mathrm{V}_j \nabla \mathrm{W}(\mathbf{r}_i - \mathbf{r}_j, l), \tag{3}$$

$$\frac{D\mathbf{u}_i}{Dt} = -\boldsymbol{g}\sum_{j=1}^{N} \mathrm{V}_j \nabla \mathrm{W}(\mathbf{r}_i - \mathbf{r}_j, l) + \boldsymbol{g}(S_0 - S_\mathrm{f})_i, \tag{4}$$

where i and j are the indices, N the total number of neighbouring particles. V the volume of the particles, W the kernel function, $\mathbf{r}$ position of the particles and l corresponds to the support length. Mathematical operator ∇ represents the gradient of the function.

Also, the particle masses are conserved as SPH follows the Lagrangian kinematic approach. Thus, the continuity equation is implicitly satisfied. Therefore, water depth h can also be estimated using an SPH approximation.

$$h(\mathbf{r}_i) = \sum_{j=1}^{N} V_j W_{ij}. \tag{5}$$

In this study, eqs (4) and (5) are used to simulate the flow field.

Kernel function

The kernel function must satisfy the symmetric and anti-symmetric gradient property. The following cubic spline function (eq. (6)) is used as the kernel function.

$$W(\mathbf{r}_i - \mathbf{r}_j, l) = \begin{cases} 1 - 1.5q^2 + 0.75q^3 & \text{if } 0 \le q < 1 \\ 0.25(2-q)^3 & \text{if } 1 \le q < 2, \\ 0 & \text{if } q \ge 2 \end{cases} \tag{6}$$

where $q = \|\mathbf{r}_i - \mathbf{r}_j\|/l$.

Note that the cubic spline function is accurate and efficient compared to other kernel functions[3]. In addition, it has a compact searching domain.

Artificial viscosity

Artificial viscosity is used to control the oscillations due to numerical solution[9].

$$\Pi_{ij} = \begin{cases} -\alpha \bar{c}_{ij} \mu_{ij} + \beta \bar{c}_{ij} \mu_{ij}^2 & \text{if } (\mathbf{u}_i - \mathbf{u}_j)\cdot(\mathbf{r}_i - \mathbf{r}_j) < 0 \\ 0 & \text{elsewhere} \end{cases} \tag{7}$$

where α and β are constants, $\bar{c}_{ij}$ the average sound speed associated with particles i and j, and $\mu_{ij} = l(\mathbf{u}_i - \boldsymbol{u}_j)\cdot(\mathbf{r}_i - \mathbf{r}_j)/((\mathbf{r}_i - \mathbf{r}_j)^2 + \varepsilon^2)$. The term involving α introduces shear and bulk viscosity, while and the term involving β handles the shock. In this study, the parameters α and β were taken as 2 and 0 respectively.

Using this damping term, the SPH shallow water momentum equation becomes

$$\frac{D\mathbf{u}_i}{Dt} = -\sum_{j=1}^{N} V_j (\boldsymbol{g} + \Pi_{ij}) \nabla W(\mathbf{r}_i - \mathbf{r}_j, l) + \boldsymbol{g}(S_0 - S_\mathrm{f})_i. \tag{8}$$

Source term

The source term in eq. (8) is modelled as given by eqs (9) and (10) below[23,24,32]. The channel bathymetry and slope can be approximated by eqs (9) and (10) respectively. The friction slope term can be calculated using the flow properties of the fluid particles using eq. (11) below.

$$Z_i = \sum_{j=1}^{N} b_j V_j W(\mathbf{r}_i - \mathbf{r}_j, l), \tag{9}$$

$$\nabla \mathrm{Z}_i = \sum_{j=1}^{N} b_j V_j \nabla W(\mathbf{r}_i - \mathbf{r}_j, l) = S_{0i}, \tag{10}$$

$$S_{f_i} = \frac{\mathbf{u}_i |\mathbf{u}_i| n_i^2}{h_i^{4/3}}, \tag{11}$$

where n is the Manning's coefficient, and b and Z represent the elevation of particles and channel bottom respectively.

Support length

The accuracy of the numerical simulation using the SPH method depends on the choice of the kernel function and its support length. If the support length is too small, there may not be enough particles in the support domain, resulting in lower accuracy. If the support length is too large, the sharp features of the solution may be smoothed out. In this study, the optimum value of support length was chosen by sensitivity analysis for the kernel used.

Also, in the SPH methodology, each particle has its own support length, which can vary in space and time according to eq. (12).

$$l = l_0 \left(\frac{h}{h_0} \right), \tag{12}$$

where l_0 and h_0 are the initial support length and water depth respectively. The domain of influence can be determined by eq. (12).

Boundary conditions

The SPH particles do not remain at a fixed position due to their Lagrangian behaviour. Two types of boundary particles have been used in this study: (1) the virtual or ghost particles[33] and (2) the inflow–outflow particles[34]. Note that the boundary particles affect the fluid particles, while the fluid particles do not affect the boundary particles.

For a solid wall boundary, the boundary particles were added outside the boundary up to a distance equal to the support radius of the fluid particles. The positions of these boundary particles were kept fixed, and they were used only in the summation for particle approximation (Figure 1). For free-slip boundary condition, the value of the tangential component of velocity of a virtual particle was taken equal to that of the nearest fluid particle, and the normal component of velocity was taken opposite to that of the nearest fluid particle. Other associated properties of these boundary particles were taken as equal to the magnitude of the same property of the nearest fluid particle. In case of a no-slip boundary condition, both normal and tangential components of velocity were taken opposite/negative to that of the nearest fluid particle.

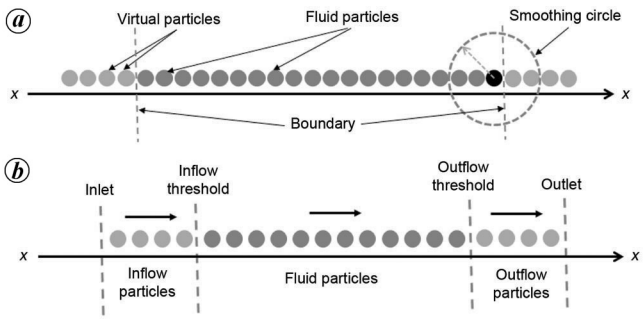

Figure 1. Boundary particles: (***a***) ghost boundary particles and (***b***) inflow/outflow boundary particles.

For the inflow and outflow conditions, two sets of boundary particles were used, one at the inlet and the other at the outlet of the flow domain. The flow moved along the longitudinal axis and was restricted by the inlet and outlet boundaries. The particles located between the inlet point and inlet threshold were treated as inflow particles. Similarly, the particles between the outflow threshold and outlet point were treated as outflow particles. An inflow particle that crosses the inlet threshold becomes a fluid particle. At the same time, a new inflow particle is generated at the inflow region to replace the exited particle. Similarly, a fluid particle that passes the outlet threshold becomes an outflow particle. Any outflow particle that crosses the outlet is deleted. Using these boundary particles, velocity and depth can be imposed at the inlet and/or outlet.

Time integration

An explicit leap-frog time discretization technique has been used to integrate particle position and velocity with time. In this scheme, the velocity and position of a particle i can be obtained as follows

$$\mathbf{r}_i = \mathbf{r}_{i-1} + \mathbf{u}_{i-1/2} \Delta t, \tag{13}$$

$$\boldsymbol{a}_i = F(\mathbf{r}_i), \tag{14}$$

$$\mathbf{u}_{i+1/2} = \mathbf{u}_{i-1/2} + \boldsymbol{a}_i \Delta t, \tag{15}$$

where Δt is the time step and $\boldsymbol{a}$ is the acceleration.

The time step should satisfy the Courant–Friedrichs–Lewy (CFL) stability condition to keep the simulation stable even in the presence of shock waves[24]. Therefore, the time step Δt was computed using CFL stability condition which depends on the support length l and sound speed c.

$$\Delta t \le \text{CFL} * \min \left(\frac{l}{(|\mathbf{u}| + c)} \right). \tag{16}$$

In this study, all computations have been performed using Intel core i7 processor with 3.07 GHz speed and 16 GB installed RAM.

Sensitivity analysis

The SPH technique involves three important parameters, i.e. initial particle number, kernel function and support radius in its formulation. To determine the appropriate number of initial particles, suitable kernel function and optimal support radius sensitivity and convergence analysis was performed considering the one-dimensional rectangular frictionless rigid bed dam break flow problem with wet bed condition. The obtained numerical results were compared with the analytical solution[35] and quantified in terms of L_2 error norm[24] as deviation from the analytical solution, and have been reported elsewhere. From the results of the sensitivity analysis, the values of the parameters were fixed for the numerical experiments. The initial number of particles was also analysed for convergence study. For the flow variable ϕ, the L_2 error norm is defined as

$$L_2(\phi) = \sqrt{\frac{1}{N}\sum_{i=1}^{N}\left(\frac{\phi_i - \phi_i^e}{\phi_i^N}\right)^2}, \quad (17)$$

where ϕ_i and ϕ_i^e are the numerical and exact solution for the ith particle respectively, and ϕ_i^N represents the normalization factor. For water depth, $\phi_i^N = h_i^e$ and for velocity, $\phi_i^N = \sqrt{gh_i^e}$ are taken to calculate the L_2 error norm.

From the sensitivity and convergence analysis, it was found that the number of initial particles should be such that the minimum spacing between them is 0.025 m for problems without bed discontinuity and 0.01 m for problems with bed discontinuity, and the support radius is two times the initial particle spacing for better accuracy and efficiency. The cubic spline function was found to be accurate and efficient.

Table 1. Initial number of particles for test problems

Problem	Number of particles
Dam break flow on a dry bed	674
Dam break flow on a wet bed	8000
Dam break flow over a step	2000
Steady flow over a step	2000
Flow over a parabolic hump	400
Hydraulic jump	400
Flow in a Parshall flume	890

Table 2. Computational time for unsteady flow problems

Problem	Simulation time (sec)			
Dam break flow on a dry bed	0.5	1.0	1.5	2.0
	11.14	20.76	30.05	39.08
Dam break flow on a wet bed	6.0	–	–	–
Initial depth ratio: 0.1	142.63	–	–	–
Initial depth ratio: 0.25	129.05	–	–	–
Initial depth ratio: 0.5	120.12	–	–	–
Dam break flow over a step	1.0	–	–	–
	40.94	–	–	–

Numerical applications

The present SPH model was applied to simulate open channel flow problems to demonstrate its capability. Both steady and unsteady flow problems were considered. Various information available at the boundary location cannot be transferred to the fluid using a single type of boundary condition. Therefore, two different approaches were employed to impose the boundary conditions. The ghost or virtual boundary particles were used as boundary conditions in unsteady flow problems. The inflow and outflow boundary particles were used in steady flow boundaries. Table 1 shows the initial particle numbers used in the simulations. The variations in the initial number of particles for different problem cases are due to the acceptable level of accuracy in the obtained results. Moreover, the problems with discontinuity in channel bed and complex geometry also require a larger number of initial particles. Table 2 shows the computational time for unsteady flow problems.

Dam break flow on a dry bed

Simulations for conditions used by LaRocque *et al.*[36] were performed for dam-break flow analysis on the dry bed downstream. The channel considered was a rectangular, frictionless, rigid bed channel. The total length of the channel was 7.3 m and the dam was located at 3.37 m distance from the furthest upstream reservoir. The initial depth of water in the reservoir was 0.25 m before the breaking of the dam. The water surface profiles in Figure 2 indicate that the present simulations are comparable to earlier experimental[36] and analytical[37,38] results. As a measure of difference from the available solution, the L_2 error norm for water surface profiles for the simulation was also obtained; the maximum values were 0.0982 and 0.158 for the analytical and

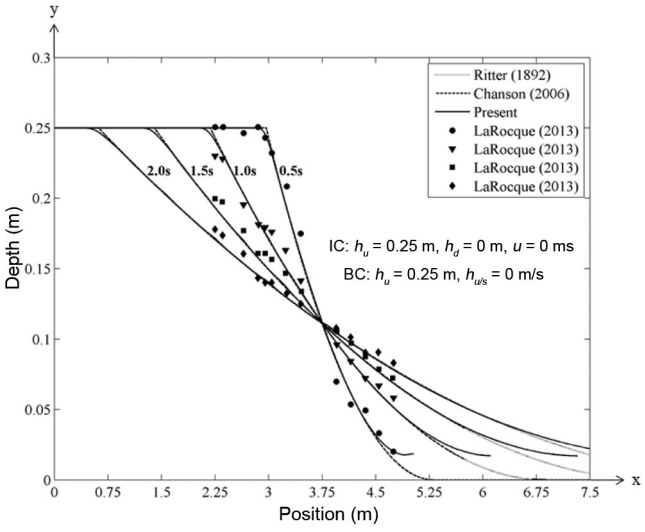

Figure 2. Dam break flow on dry bed.

experimental results, respectively. The positive surge front was under-predicted. This may be attributed to the frictionless assumption of the channel bed in the simulations.

Dam break flow on a wet bed

Simulation for the wet downstream dam break flow was done for $t = 6$ sec after the breaking of the dam, and it was assumed that the dam breaks instantaneously at $t = 0$ sec. The channel considered for this test case was a rectangular, smooth channel of length 200 m; and the dam section was located in the middle of the channel prior to the dam break.

Three different initial depth ratios (i.e. h_d/h_u) 0.1, 0.25 and 0.5 were considered. $h_u = 10$ m for all the cases. The obtained results from simulations for water surface profiles along with the analytical solution in Figure 3 show that the surge waves travelling both upstream and downstream are similar to the analytical solution[35].

In the dam break flow, the entire flow field of the channel remains subcritical when the initial water depth ratio is greater than 0.138; while the flow field downstream of the dam remains supercritical and upstream remains subcritical for the initial water depth ratio lower than 0.138 (ref. 21), which has been verified in present simulations.

The maximum L_2 error norm for water surface profiles in this test case was found to be 0.038.

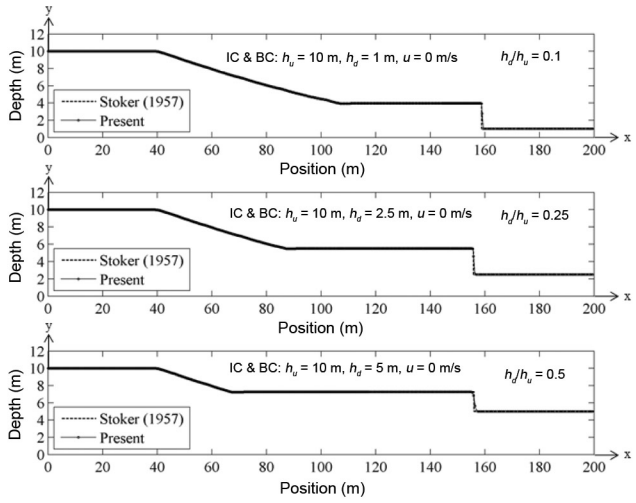

Figure 3. Dam break flow on a wet bed.

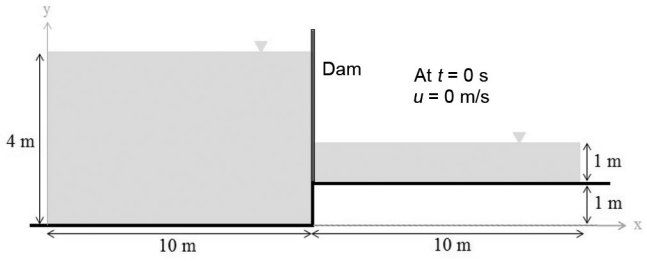

Figure 4. Geometry and initial configuration of dam break flow over a step.

Dam break flow over a step

This test problem involves both bottom and free surface discontinuities as initial conditions (Figure 4). Thus, the source terms need to be discretized accurately[32]. A rectangular channel with a smooth rigid bed has been considered. The channel bed configuration was taken as $b = 0$ m for $x < 10$ m and $b = 1$ m for $x \geq 10$ m. All the particles were at rest when the dam broke instantaneously at $t = 0$ sec. The obtained results for the surface profile closely agreed with the analytical solution (Figure 5). However, there was a small discrepancy near the sharp discontinuity across the step. The movement of positive and negative surge waves has been well captured by the model. The flow characteristics were found to be subcritical in the entire channel section. The L_2 error norm statistics between the simulated and analytic surface profiles were equal to 0.219, and the overall accuracy of the simulated results was acceptable.

Steady flow over a step

This test case was chosen to predict the model's capability in capturing the surface and velocity profiles in case of steady flows. The channel configuration for this test was similar to the above problem. The total length of the channel was 20 m and the discontinuity in the bed was located at the middle of the channel. In the simulation, constant discharge, $Q = 4.821$ m^3/sec was provided at the inlet boundary by imposing a constant water depth equal to 3.4 m and a constant velocity equal to 1.419 m/sec. At the outlet, a water depth equal to 3.27 m was imposed. Comparison between the present results and available solution[32] indicates that they are in close agreement, except for water surface elevation across the step (Figure 6). The obtained L_2 error norm

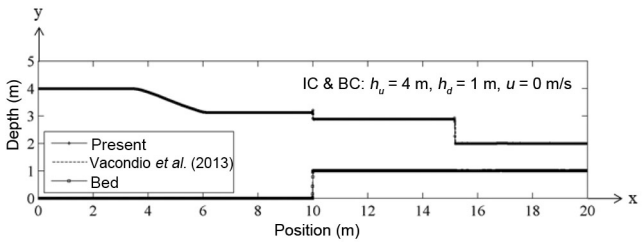

Figure 5. Dam break flow over a step at $t = 1$ s.

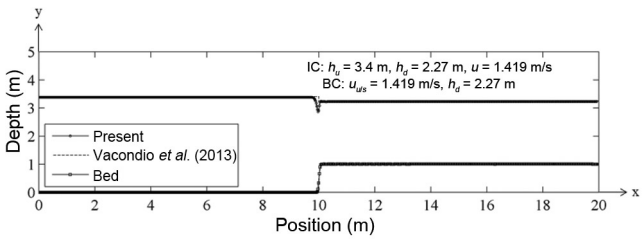

Figure 6. Steady state flow over a step.

statistics for the overall prediction of the surface profile was 0.19 and was found to be satisfactory.

Flow over a parabolic hump

Steady flow over a hump has been studied by many researchers to verify their numerical models[24,39], as the analytical solution is available for these tests. A rectangular, rigid bed smooth channel was used. The profile of the hump is characterized by

$$b(x) = \begin{cases} b_0\left[1 - \dfrac{(x-5)^2}{4}\right] & \text{if } 3 \text{ m} < x < 7 \text{ m} \\ 0 & \text{elsewhere} \end{cases} \quad (18)$$

where x represents the distance along the channel and b_0 = 0.2 m.

The flow over the channel can be subcritical, transcritical or supercritical depending on the inflow and outflow boundary conditions. Therefore, a total of three sub-cases were simulated by imposing different inflow and outflow boundary conditions. Table 3 shows the type of flow obtained in the simulation and imposed boundary conditions for all three sub-cases. Boundary condition was imposed by the inflow–outflow boundary particles[34]. Figure 7 shows the simulated water surface profiles for the three sub-cases at a steady state along the channel. The obtained results for sub-cases 1 and 3 are in good agreement with the analytical solution. However, small discrepancies are present near the shock in the simulated results of sub-case 2. Similar results have also been reported by Vacondio *et al.*[24]. The obtained maximum L_2 error norm statistics of 0.049 for the same justifies the numerical accuracy of the simulated results of the present numerical model.

Table 3. Imposed boundary conditions for flow over a parabolic hump

Case	Flow	Upstream boundary conditions (m/sec)	Downstream boundary conditions (m)
I	Supercritical	4.000	0.10
II	Transcritical	0.435	0.33
III	Transcritical	0.435	0.10

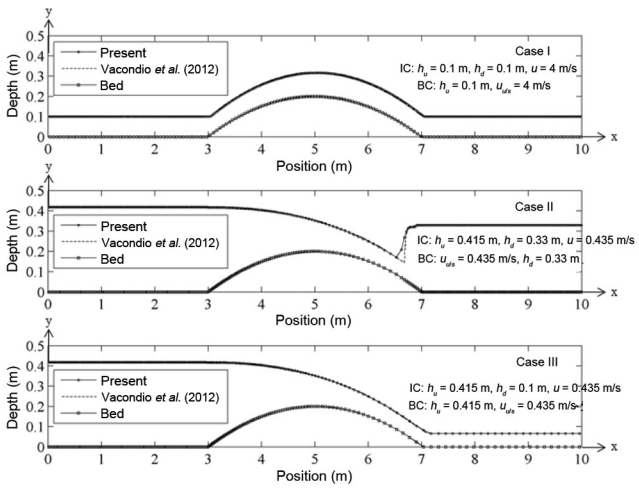

Figure 7. Flow over a parabolic hump.

Hydraulic jump

Simulations were performed for inflow Froude numbers (F_{r1}) ranging from 2.3 to 7.0, and the obtained results were compared with the experimental results of Gharangik and Chaudhry[40]. In the simulations, constant discharge was maintained at the upstream inflow boundary and a constant water depth was enforced at the outlet. The initial conditions used by Gharangik and Chaudhry[40] were also used in our simulations.

Figure 8 shows simulated hydraulic jump profiles for four different F_{r1} values. The jump is characterized by a rise in water surface elevation. The discontinuity between the inflow and outflow velocities in the supercritical and subcritical regimes generates shock waves that propagate downstream. Initially, the wavefronts move downstream for a small time interval. Thereafter, they move upstream for the remaining simulation time. Due to the one-dimensional formulation and smoothing effect of the SPH method, the present model is unable to capture the rollers. However, the oscillating characteristics of the fronts are captured by the model. The jump profile was better simulated at lower than higher Froude numbers. The obtained maximum L_2 error norm statistics of 0.178 for this study show that the behaviour of the hydraulic jump is well represented by the SPH model.

Flow in a Parshall flume

A simulation was performed for the study case conducted at the University of Windsor (Ontario, USA) in a Parshall flume[41] (Figure 9). Discharge, Q = 0.0145 m^3/sec was maintained at the inlet boundary at all times.

Figure 10 shows the simulated results of the present SPH model for transcritical flow in the Parshall flume. The cross-channel averaged experimental and numerically predicted flow surface profiles along the centreline of the flume were compared. The model did not capture the flow transition from subcritical to supercritical state accurately. However, the flow behaviour closely resembled the actual cross-channel averaged flow profile. For the upstream flow region, the agreement between experimental and numerical results was good. However, discrepancies between the simulated and experimental results could be observed downstream of the converging section of the flume. In this flow region, the model slightly overestimated the water surface elevation. The flow characteristics were found to be in transition from subcritical to supercritical flow. The accuracy

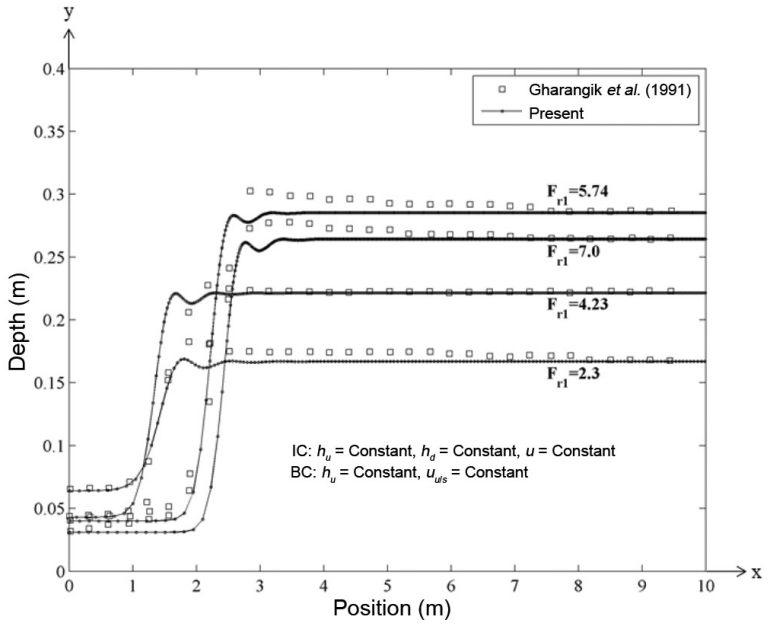

Figure 8. Variation of hydraulic jump profile with inlet Froude number.

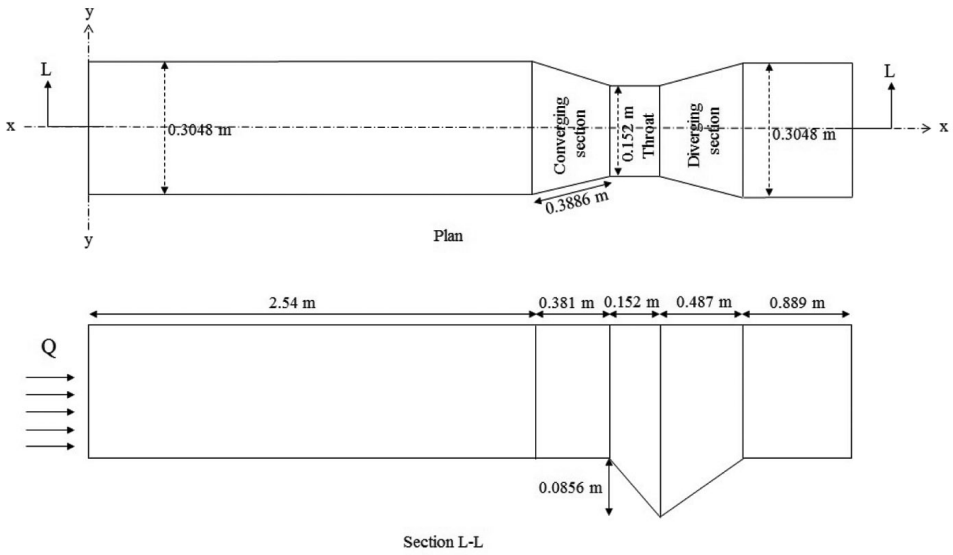

Figure 9. Geometry and configuration of a Parshall flume.

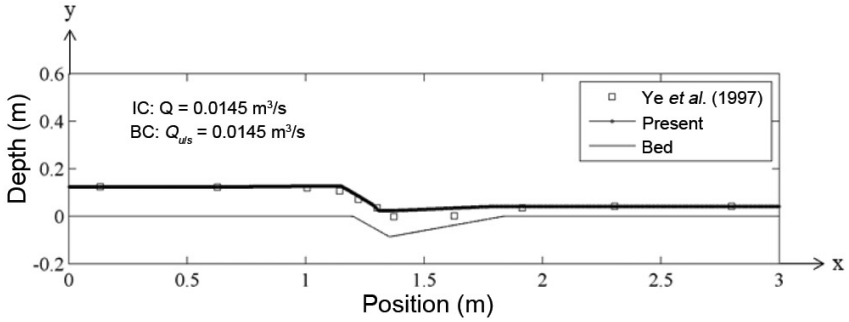

Figure 10. Steady flow surface profile in a Parshall flume.

in the simulation of the surface profile with respect to experimental data in terms of L_2 error norm was 0.341.

Conclusion

In this study, an SPH model using SWEs has been presented. The bed discontinuity was modelled using fluid particles to reduce computational costs in the simulation. The sensitivity and convergence analysis was performed to determine the model parameters. The numerical accuracy of simulated results was also quantified in terms of L_2 error norm with respect to results available in the literature. Seven different open channel flows were simulated using the developed SPH model. Results indicate that this method can be used as a reliable tool to simulate open-channel flows.

SWEs with source terms were numerically solved using the SPH method. The proposed model could use the inflow and outflow boundaries accurately. In addition, bed discontinuity was modelled using the fluid particles without any extra bed particles. Artificial viscosity to smoothen the numerical oscillations in water surface profiles was considered. Optimal model parameters were obtained by sensitivity and convergence analysis. Several open channel flows (with varying complexities) were simulated to demonstrate the model capability. The numerical accuracy for all results was quantified in terms of L_2 error norm. Comparison with earlier results indicates that the SPH model can be used as a tool to study open channel flows on a rigid bed. It can accurately compute the water surface profiles, including capturing shocks in flood wave propagation and can be effectively used for open channel flows on beds having discontinuities. However, there are small discrepancies in some of the obtained results due to function approximations by the kernel function which has a smoothening effect. Moreover, the present study focuses on one-dimensional solutions to these problems. In reality, the open channel flow problems are typically three-dimensional. Thus, the one-dimensional approximation of the three-dimensional problems and the smoothing effect of the SPH formulation may be the reasons for small discrepancies in the simulated results.

In addition, we present a one-dimensional numerical model based on the SPH methodology. It can simulate the flow fields of one-dimensional open-channel flow problems with or without channel bed discontinuity. However, for multi-dimensional flow problems, the dimensionality of the model should be extended for better results. The developed model is also for rigid bed flows. To include the transport of sediments and/or pollution, etc. the respective transport models can be considered along with the proposed model. Moreover, this model cannot estimate the flow profiles of highly turbulent flow accurately since it does not have a turbulence flow module. For simulating highly turbulent flow, turbulence models like the k–ε model can be incorporated.

1. Chaudhry, M. H., *Open Channel Flow*, Springer, New York, USA, 2008, 2nd edn.
2. Cunge, J. A., Holly, F. M. and Verwey, A., *Practical Aspects of Computational River Hydraulics*, Pitman Advanced Publishing Program, London, UK, 1980, p. 420.
3. Liu, G. R. and Liu, M. B., *Smoothed Particle Hydrodynamics: AMeshfree Particle Method*, World Scientific Publishing, Singapore, 2003.
4. Wang, Z. and Shen, H. T., Lagrangian simulation of one-dimensional dam-break flow. *J. Hydraul. Eng*., 1999, **125**(11), 1217–1220.
5. Monaghan, J. J., Smoothed particle hydrodynamics. *Rep. Progress Phys.*, 2005, **68**(3), 1703–1759.
6. Monaghan, J. J., Smoothed particle hydrodynamics. *Ann. Rev. Fluid Mech*., 2012, **44**, 323–346.
7. Gomez-Gesteira, M., Rogers, B. D., Dalrymple, R. A. and Crespo, A. J. C., State of the art of classical SPH for free-surface flows. *J. Hydraul. Res*., 2010, **48**(1), 6–27.
8. Violeau, D. and Rogers, B. D., Smoothed particle hydrodynamics (SPH) for free-surface flows: past, present and future. *J. Hydraul. Res*., 2016, **54**(1), 1–26.
9. Monaghan, J. J., Simulating free surface flows with SPH. *J. Comput. Phys*., 1994, **110**(2), 399–406.
10. Swegle, J. W., Hicks, D. L. and Attaway, S. W., Smoothed particle hydrodynamics stability analysis. *J. Comput. Phys*., 1995, **116**(1), 123–134.
11. Morris, J. P., Fox, P. J. and Zhu, Y., Modelling low Reynolds number incompressible flows using SPH. *J. Comput. Phys*., 1997, **136**(1), 214–226.
12. Bonet, J. and Lok, T. S. L., Variational and momentum preservation aspects of smoothed particle hydrodynamics formulations. *Comput. Methods Appl. Mech. Eng*., 1999, **180**(1–2), 97–115.
13. Cummins, S. J. and Rudman, M. J., An SPH projection method. *J. Comput. Phys*., 1999, **152**(2), 584–607.
14. Inutsuka, S. I., Reformulation of smoothed particle hydrodynamics with Riemann solver. *J. Comput. Phys*., 2002, **179**(1), 238–267.
15. Cha, S. H. and Whitworth, A. P., Implementations and tests of Gudunov-type particle hydrodynamics. *Mon. Notice R. Astro. Soc.*, 2003, **340**, 73–90.
16. Rodriguez-Paz, M. and Bonet, J., A corrected smooth particle hydrodynamics formulation of the shallow-water equations. *Comput. Struct*., 2005, **83**(17–18), 1396–1410.
17. Hu, X. Y. and Adams, N. A., A multi-phase SPH method for macroscopic and mesoscopic flows. *J. Comput. Phys*., 2006, **213**(2), 844–861.
18. Grenier, N., Antuono, M., Colagrossi, A., Le-Touze, D. and Alessandrini, B., A Hamiltonian interface SPH formulation for multi-fluid and free surface flows. *J. Comput. Phys*., 2009, **228**(22), 8380–8393.
19. De-Leffe, M., Le-Touze, D. and Alessandrini, B., SPH modeling of shallow-water coastal flows. *J. Hydraul. Res*., 2010, **48**(1), 118–125.
20. Vila, J. P., On particle weighted methods and smoothed particle hydrodynamics. *Math. Models Methods Appl. Sci.*, 1999, **9**(2), 161–209.
21. Chang, T. J., Kao, H. M., Chang, K. H. and Hsu, M. H., Numerical simulation of shallow-water dam break flows in open channels using smoothed particle hydrodynamics. *J. Hydrol*., 2011, **408**(1–2), 78–90.
22. Kao, H. M. and Chang, T. J., Numerical modeling of dam break-induced flood and inundation using smoothed particle hydrodynamics. *J. Hydrol*., 2012, **448**, 232–244.
23. Vacondio, R., Rogers, B. D. and Stansby, P. K., Accurate particle splitting for smoothed particle hydrodynamics in shallow water with shock capturing. *Int. J. Numer. Methods Fluids*, 2012, **69**(8), 1377–1410.
24. Vacondio, R., Rogers, B. D., Stansby, P. K. and Mignosa, P., SPH modeling of shallow flow with open boundaries for practical flood simulation. *J. Hydraul. Eng*., 2012, **138**(6), 530–541.

25. Meister, M., Burger, G. and Rauch, W., On the Reynolds number sensitivity of smoothed particle hydrodynamics. *J. Hydraul. Res*., 2014, **52**(6), 824–835.
26. Sun, P. N., Colagrossi, A., Marrone, S. and Zhang, A. M., The δ plus-SPH model: simple procedures for a further improvement of the SPH scheme. *Comput. Methods Appl. Mech. Eng*., 2017, **315**, 25–49.
27. Chang, K. H., Sheu, T. W. H. and Chang, T. J., A 1D–2D coupled SPH–SWE model applied to open channel flow simulations in complicated geometries. *Adv. Water Resour*., 2018, **115**, 185–197.
28. Gu, S., Bo, F., Luo, M., Kazemi, E., Zhang, Y. and Wei, J., SPH simulation of hydraulic jump on corrugated riverbeds. *Appl. Sci.*, 2019, **9**(3), 436.
29. Hsu, T. W., Liang, S. J. and Wu, N. J., Application of meshless SWE model to moving wet/dry front problems. *Eng. Comput*., 2019, **35**(1), 291–303.
30. Hsu, T. W., Liang, S. J. and Wu, N. J., A 2D SWE meshless model with fictitious water level at dry nodes. *J. Hydraul. Res*., 2021, **59**(6), 917–931.
31. Chang, K. H., Chang, T. J. and Garcia, M. H., A well-balanced and positivity-preserving SPH method for shallow water flows in open channels. *J. Hydraul. Res*., 2021, **59**(6), 903–916.
32. Vacondio, R., Rogers, B. D., Stansby, P. K. and Mignosa, P., A correction for balancing discontinuous bed slopes in two-dimensional smoothed particle hydrodynamics shallow water modeling. *Int. J. Numer. Methods Fluids*, 2013, **71**(7), 850–872.
33. Ferrari, A., Dumbser, M., Toro, E. F. and Armanini, A., A new 3D parallel SPH scheme for free surface flows. *Comput. Fluids*, 2009, **38**(6), 1203–1217.
34. Federico, Marrone, S., Colagrossi, A., Aristodemo, F. and Antuono, M., Simulating 2D open-channel flows through an SPH model. *Eur. J. Mech. B/Fluids*, 2012, **34**, 35–46.
35. Stoker, J. J., *Water Waves: Mathematical Theory with Applications*, Wiley-Interscience, Singapore, 1957.
36. LaRocque, L. A., Imran, J. and Chaudhry, M. H., Experimental and numerical investigations of two dimensional dam break flows. *J. Hydraul. Eng*., 2013, **139**(6), 569–579.
37. Ritter, A., The propagation of water waves. *Ver Deut. Ing.-Z*., 1982, **36**(33), 947–954.
38. Chanson, H., Analytical solutions of laminar and turbulent dam break wave. In Proceedings of the International Conference on Fluvial Hydraulics River Flow, Taylor and Francis, London, 2006, pp. 465–474.
39. Aureli, F., Maranzoni, A., Mignosa, P. and Ziveri C., A weighted surface–depth gradient method for the numerical integration of the 2D shallow water equations with topography. *Adv. Water Resour*., 2008, **31**(7), 962–974.
40. Gharangik, A. M. and Chaudhry, M. H., Numerical simulation of hydraulic jump. *J. Hydraul. Eng*., 1991, **117**(9), 1195–1211.
41. Ye, J. and McCorquodale, J. A., Depth averaged hydrodynamic model in curvilinear collocated grid. *J. Hydraul. Eng*., 1997, **123**(5), 380–388.

Received 5 May 2022; revised accepted 14 February 2023

doi: 10.18520/cs/v124/i12/1422-1430